

Time-reversed Young’s experiment: Deterministic, diffractionless second-order interference effect

Jianming Wen^{1,*}

¹*Department of Electrical and Computing Engineering,
Binghamton University, Binghamton, New York 13902, USA*

(Dated: December 24, 2024)

The classic Young’s double-slit experiment exhibits first-order interference, producing alternating bright and dark fringes modulated by the diffraction effect of the slits. In contrast, here we demonstrate that its time-reversed configuration produces an ideal, deterministic second-order ‘ghost’ interference pattern devoid of diffraction and first-order effect, with the size dependent on the dimensions of the ‘effectively extended light source.’ Furthermore, the new system enables a range of effects and phenomena not available in traditional double-slit interference studies, including the formation of programmed and digitized interference fringes and the coincidence of the pattern plane and the source plane. Despite the absence of first-order interference, our proposed experiment does not rely on nonclassical correlations or quantum entanglement. The elimination of diffraction through time-reversal symmetry holds promise for advancing superresolution optical imaging and sensing techniques beyond existing capabilities.

Young’s double-slit experiment stands as a cornerstone in modern physics, bearing profound implications for our comprehension of the nature of light and matter. Originally conducted by Thomas Young [1] in the early nineteenth century, this seminal experiment provided compelling evidence for the wave-like attributes of light through the observation of interference patterns produced by light traversing two closely spaced slits. This groundbreaking revelation challenged the prevalent notion of light solely as a particle and laid the foundation for the wave-particle duality [2–12] concept—a keystone principle of quantum mechanics. Moreover, Young’s experiment elucidated the principles of superposition and coherence, bedrock tenets underpinning various domains of modern physics, including quantum mechanics and optics. Its significance transcends the realm of light, as similar interference phenomena have been observed with matter waves [13–24], reinforcing the unified nature of physics and complementarity interpretation of quantum mechanics. Thus, Young’s interference experiment remains indispensable in molding our understanding of the fundamental principles governing the behavior of light and matter, with far-reaching implications across diverse fields of scientific inquiry.

On the other hand, the diffraction effect assumes a pivotal role in Young’s experiment, broadening our comprehension of wave behavior while simultaneously posing challenges in experimental precision. Positively, diffraction is intrinsic to the creation of the interference pattern observed in the experiment. As light passes through an aperture, it diffracts and spreads out into a succession of wavefronts. According to the Huygens-Fresnel principle, these wavefronts superpose and interfere with each other, engendering regions of constructive and destructive interference, which form the characteristic bright and dark fringes on the screen. Meanwhile, diffraction can present challenges in experimental setup and inter-

pretation. The dispersion of light due to diffraction can obscure the interference pattern, diminishing the sharpness of the fringes and complicating measurements. Additionally, diffraction around the edges of the slits introduces high order maxima and minima, thereby confining the observable scale of the interference pattern. Despite these challenges, understanding and accounting for the diffraction effect are essential for accurate interpretation and application of the results derived from traditional Young’s experiment.

Here, we show that by substituting the original point light source with a position-fixed point (or bucket) detector and replacing the observation plane with a spatially extended point-light-emitter source in the standard double-slit experiment, a novel time-reversed configuration unveils a variety of peculiar phenomena characterized by counter-intuitive effects unattainable with the classic Young’s experiment. Notably, one such phenomenon is the emergence of diffractionless deterministic interference fringes, where the lateral dimensions of the entire light source determine the size of the pattern, alongside the potential for programmable or digitised interference formation. Another noteworthy aspect is that the underlying physics of this setup diverges fundamentally from established knowledge, as the phenomenon inherently pertains to the two-particle second-order correlation effect, with its interpretations contrasting conventional single-particle picture developed from the statistical Young’s experiment. We anticipate that our discoveries will deepen understanding of the renowned double-slit experiment and pave the way for the development of new superresolution imaging and sensing technologies in the post-diffraction era.

To facilitate our discussion, we begin by standardizing our notation with a brief overview of Young’s experiment. In its classic setup, as depicted in Fig. 1(a), two narrow slits, A and B, each with a width w and separated by

a distance d , are illuminated by a point monochromatic light source S (solid circle). This source emanates an optical field E at wavelength λ and wavenumber $k = 2\pi/\lambda$ and is positioned at a distance l along the optical x -axis from the origin O . The irradiance at point $P(L, y)$ on the observation screen V , located at a distance L from the plane containing A and B , is determined by the superposition of the overall fields after two slits,

$$E_P = E_A + E_B, \quad (1a)$$

$$E_A = \frac{E e^{ikr_{SA}}}{r_{SA}} \int_{\frac{d-w}{2}}^{\frac{d+w}{2}} ds \frac{e^{ikr_{AP}}}{r_{AP}}, \quad (1b)$$

$$E_B = \frac{E e^{ikr_{SB}}}{r_{SB}} \int_{-\frac{d-w}{2}}^{-\frac{d+w}{2}} ds \frac{e^{ikr_{BP}}}{r_{BP}}. \quad (1c)$$

To simplify the discussion, hereafter we will concentrate on the case of the paraxial approximation with $r_{SA} = r_{SB} \simeq l$ and $r_{AP} = r_{BP} \simeq L + d^2/8L - ys/L$. Note that the optical path differentiation ys/L is much smaller than L , so it can be disregarded in the amplitude factors in Eqs. (1b) and (1c) to the lowest order. However, this path difference cannot be neglected in the phase factors. Consequently, the irradiance at $P(L, y)$ is computed by

$$I(y) = \frac{\epsilon_0 c}{2} |E_P|^2 = 4I_0 \text{sinc}^2 \left(\frac{\pi w}{\lambda L} y \right) \cos^2 \left(\frac{\pi d}{\lambda L} y \right), \quad (2)$$

where $I_0 = \epsilon_0 c w^2 |E|^2 / 2l^2 L^2$ with c being the speed of light in vacuum and ϵ_0 the permittivity of vacuum. This characteristic shape of Young's diffraction-interference intensity profile is illustrated in Fig. 1(b), using a 500-nm cw laser to illuminate a double-slit with $w = 0.15$ mm, $d = 0.5$ mm, and $L = 0.8$ m as an example. However, when an extended light source (dashed hollow circles) with a lateral dimension of σ is introduced, the distinct interference fringes tend to blur and becomes diffused if $d\sigma/l > \lambda/2$, thereby establishing the spatial coherence criteria for an extended light source [25].

Several critical conclusions can be readily drawn from Eq. (2): (i) The resulting interference-diffraction structure, $I(y)$, is distributed 'locally' on the observation screen V and depends on the geometrical parameters (L, y) extending from the double-slit plane to V , while remaining unaffected by the geometrical parameter l from the source S to the origin O . (ii) The extent of observable interference fringes is controlled by the diffraction effect originating from the slit aperture. (iii) The source S and the observation screen V are situated on opposite sides of the double-slit plane. (iv) Each point on the interference pattern emerges probabilistically or statistically from slit diffraction and cannot be chosen at will, making it unrealistic to have a one-to-one correspondence between the source and the observation. (v) The fundamental physics behind this phenomenon can be attributed to the behavior of individual particles (i.e., the single-particle effect), as verified by feeble light illumination [2].

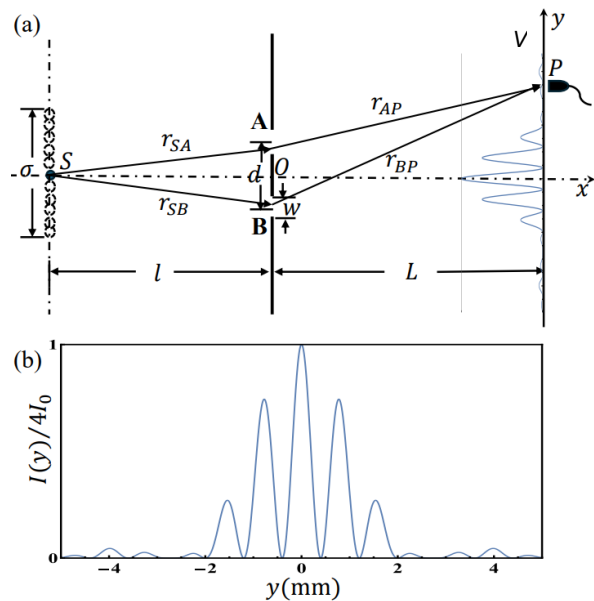


FIG. 1. (a) Schematic of the standard Young's experiment, showing that the diffraction-interference fringes and the source plane must be located on opposite sides of the double-slit plane. (b) Illustration of a typical first-order diffraction-interference pattern non-deterministically formed on the detection y -plane.

However, as we delve into the analysis below, we find that each of the aforementioned conclusions can be systematically challenged through a time-reversal configuration of the typical Young's experiment, since this time-reversed operation leads to totally nonreciprocal physics. Also in sharp contrast, in the time-reversed scheme, there is no spatial coherence requirement on the lateral scale of the source whatsoever. Specifically, we are intrigued by a new rendition of Young's double-slit experiment, wherein we replace the original point source S with a position-fixed point or bucket detector D , while concurrently substituting the observation screen V with a laterally extended light source S' , as schematic in Fig. 2(a). Through our forthcoming demonstration, we aim to highlight that despite both setups (Fig. 1(a) versus Fig. 2(a)) adhering to time-symmetry operations, they inherently diverge and engender asymmetric, non-reciprocal physical effects. Unlike the first-order 'local' diffraction-interference pattern on V (Fig. 1(b)), this time-reversed system invariably produces a second-order 'nonlocal' diffraction-free, perfect interference pattern (Fig. 2(b)) determined by the information of both source and detection, devoid of the first-order interference.

To clarify this concept, let us examine the new system schematic in Fig. 2(a) more carefully. Imagine a scenario with only one photo-detector, denoted as D , positioned at a fixed location $(L, 0)$. In this scheme, D only registers fluctuating light intensities or powers over time but lack the capability to discern the light's origin. Even

when the recorded irradiance originates from two distinguishable paths, D cannot differentiate between them. As a result, generating any meaningful pattern, including interference fringes, becomes unfeasible regardless of the spatial coherence of the light source. This observation highlights the necessity of extracting positional information from the light source to derive meaningful patterns. One potential solution is to ensure that only a single point emitter within the light source emits light at any moment, with its emission position being uniquely identifiable. How then, could we practically achieve such precise specifications?

Several strategies offer promise in this regard, providing avenues for experimenting the proposed concept:

Solution I (Sol-I): One possible way involves leveraging an ensemble of identical point light emitters, each capable of two-photon fluorescence. By ensuring that only one emitter fluoresces at any given moment, a photon from the emitted light can be directed to illuminate the double-slit aperture, while the other photon is utilized to map the emitter's position. This positional mapping could be achieved through a Gaussian thin lens imaging process, for example. Subsequently, by analyzing the photon trigger events detected by D , a nontrivial event distribution map can be generated, correlating with the positions of the individual point emitters.

Solution II (Sol-II): Another more practical approach involves the development of a programmable light source. This entails the artificial construction of a uniform array of chromatic point light sources, where each emitter can be selectively activated to radiate light onto the double slits within a synchronized timeframe. Such on-demand activation may be realizable via different means. For instance, integrated electric fields can be utilized to sequentially excite each point source, with its spatial coordinate being simultaneously recorded. Alternatively, one can employ chemical markers or electro-optical effect to excite point emitters while simultaneously labelling their coordinate positions.

Solution III (Sol-III): The third practical route is to fabricate a point source capable of precise spatial movement. To achieve this, for instance, one could affix a stable point light emitter, such as a quantum dot or an nitrogen-vacancy center in diamond, to the tip of a position-movable cantilever in such as atomic force microscopy. Then, the emitter can be laterally positioned with precision, maintaining a stationary position for an equal duration of emission at each point. As a consequence, the light intensities detected by the detector D accurately mirror the spatial dynamics of the light source's movement.

It is evident that the essential objective across these three method categories is to establish a one-to-one correspondence between the captured light and the emitting source's precise spatial coordinates at that particular instance. This bit of spatial data information, crucial for

the proposed time-reversed Young's experiment, enables the demonstration of diffractionless second-order interference by simply sorting the sequence of intensities or trigger events recorded on detector D . To facilitate this, we consider a point source S' positioned at coordinates $(-l, y')$ in Fig. 2(a), emitting light onto the double slits. Subsequently, as the light traverses the double slits, it is intercepted by D stationed at coordinates $(L, 0)$. The total electric field E_D at D now takes the form of

$$E_D = E_A + E_B, \quad (3a)$$

$$E_A = \frac{E e^{i k r_{S'A}}}{r_{S'A}} \int_{\frac{d-w}{2}}^{\frac{d+w}{2}} ds \frac{e^{i k r_{AD}}}{r_{AD}}, \quad (3b)$$

$$E_B = \frac{E e^{i k r_{S'B}}}{r_{S'B}} \int_{-\frac{d+w}{2}}^{-\frac{d-w}{2}} ds \frac{e^{i k r_{BD}}}{r_{BD}}. \quad (3c)$$

Again, under the paraxial approximation, we have $r_{S'A} \simeq l + d^2/8l - dy'/2l$, $r_{S'B} \simeq l + d^2/8l + dy'/2l$, and $r_{AD} = r_{BD} \simeq L$. Similarly, the optical path difference dy'/l is negligible in the amplitude factors in Eqs. (3b) and (3c) but cannot be neglected in the phase factors. The irradiance recorded at D then assumes the following simpler result,

$$I(y') = \frac{\epsilon_0 c}{2} |E_D|^2 = 4I_0 \cos^2 \left(\frac{\pi d}{\lambda l} y' \right), \quad (4)$$

deterministic and ideal interference fringes that depend on the y' -position of the emitting light source and remain unaffected by diffraction at all! It is intriguing how Eq. (4) appears impervious to the diffraction effect, even with the slit apertures in place. In addition, this intensity distribution is unequivocally dictated by the overall size σ' of the light source. Thanks to the position-fixed detector D , measurements are effectively unaffected by slit diffraction—a challenge commonly encountered in previous studies where fields diffract after passing through the aperture.

In contrast to $I(y)$, $I(y')$ hinges on having instantaneous positional information of a point emitter, represented by a spatial correlation $\delta(y'' - y')$ across the source plane. It is this spatial correlation in emission that distinguishes the second-order correlation (or effective 'two-particle') effect, signaling a radical departure from the single-particle perspective illustrated in standard Young's experiment. Alternatively, the $I(y')$ contour depends solely on the geometric properties from the source plane to the double-slit plane. Without the emitter's coordinate information, detector D simply records a temporal sequence of light intensities or photon trigger events, lacking the first-order interference phenomenon.

The construction of the interference fringes (4) is built upon organizing the recording data from D according to the positions of point emitters. This one-to-one correspondence enables a unique way of programming interference patterns using a programmable source like Sol-II and Sol-III as proposed above. Note that the ability

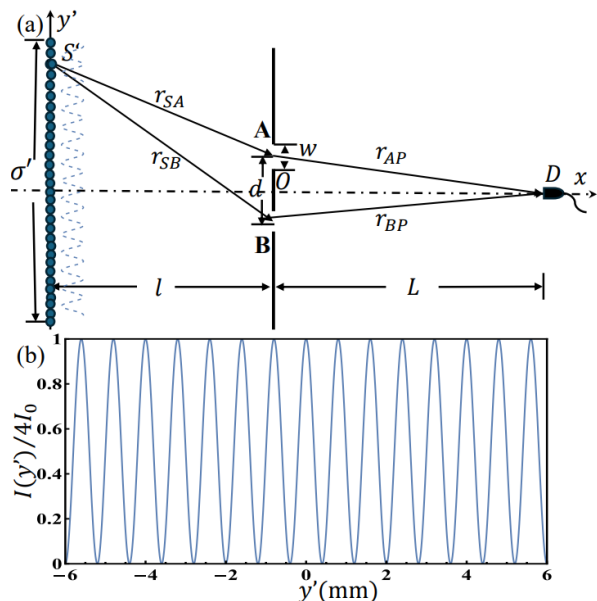


FIG. 2. (a) Schematic of the time-reversed Young's experiment, demonstrating that the nonlocal, nondiffractive interference fringes (dashed) and the source plane overlap and are located on the same side of the double-slit plane. (b) Illustration of a second-order diffractionless interference pattern deterministically formed by organizing the recorded data from a fixed-position detector D based on the position coordinates of each individual point light emitter on the y' -plane.

to form such programmable interference fringes is exclusive to the time-reversed design is beyond the capabilities of traditional double-slit setups, regardless of whether classical or quantum light sources are considered. The emitter's spatial correlation within the source plane actually erases the probabilistic relationship between emission and detection, which is however inherent in traditional arrangements due to the unavoidable diffraction effects behind the slits. From this viewpoint, the non-diffractive interference fringes (4) resemble a spatial version of a Mach-Zehnder interferometer [26–30] with single photons to some extent, but with seemingly distinct underlying physics.

On the other hand, the proposed time-reversed version must display some level of complementarity with the conventional setup. Indeed, this is evident when considering that $I(y)$ and $I(y')$ share the same intensity normalization constant I_0 . Upon comparing Eqs. (1b) and (1c) with Eqs. (3b) and (3c), it is apparent that while the spherical wavelets before the slits in Young's experiment do not directly contribute to interference formation, they are nonetheless essential for the emergence of interference patterns in the time-reversed setup. Additionally, in traditional Young's experiment (Fig. 1), the diffraction-interference effect arises precisely from the light beyond the slits, presenting a stark contrast to our time-reversed configuration where it remains constant. This further

underscores the complementary nature between the two systems, as expected.

For a deeper understanding of the process, we introduce here an advanced-wave pictorial description. In this conceptual depiction of time-reversal, a photon originates at detector D , travels back to the source, and conveys its propagation details to 'another (virtual) photon.' This 'second photon' is then 'locally detected at that position,' effectively tracing all possible trajectories of the initially transmitted photon. Alternatively, the picture implies that the source plane and the pattern plane now align with each other, marking a radical departure from prior research. The spatial correlation at the source position is instrumental in mitigating the diffraction effect during measurement. In our system, the resolution of the resultant pattern is not contingent upon light diffraction but rather relies on the precise acquisition of the position of the luminous point at the source. This feature allows us to fundamentally surpass the Rayleigh diffraction limit, offering a compelling approach to super-resolution optical imaging and sensing in biological and medical applications compared to existing methodologies based on near-field techniques (such as photon scanning tunneling microscopy [31] and superlens [32]) or on far-field methods (such as confocal microscopy [33], 4Pi microscope [34], structured-illumination microscopy [35, 36], fluorescence microscopy [37–41], and quantum optics [42–44]).

One might wonder whether our time-reversed double-slit experiment bears resemblance to the famous ghost diffraction-interference experiment [45, 46], wherein one photon from a pair of entangled photons illuminates the double-slit while being detected by a position-fixed, pointlike photon counting detector. Simultaneously, the other photon freely propagates to a spatially scanning photon counting detector, leading to the creation of non-local two-photon diffraction-interference fringes via coincidence counts. Despite both experiments falling under second-order correlation and lacking first-order interference, they are completely nonequivalent. The latter relies on quantum entanglement, particularly momentum correlation, between paired photons, whereas the former depends on spatial correlation in photon emission. Furthermore, according to Klyshko's advanced-wave picture [47], the ghost interference experiment can be interpreted as one photon being generated at a detector, traveling backward to pass through the slits and the source, where it becomes the second photon, before moving forward in time to reach the second detector. This interpretation contrasts with our explanation of the latter setup, where the 'second (virtual) photon' does not necessitate propagation to generate the pattern. Moreover, while the diffraction effect persists in the former experiment, it is entirely absent in the latter. All in all, the two experiments obey distinctive physical principles.

To summarize, the time-reversed double-slit experiment intrinsically involves a second-order correlation ef-

fect, enabling the formation of programmable [48] and deterministic interference fringes with a span determined by the lateral dimensions of an array of point emitters. Although we used light as an example to illustrate this concept, we believe that a similar setup could be extended to other substances such as electrons, atoms, and molecules. Given the numerous applications of super-resolution imaging and sensing in contemporary science, we anticipate that our diffractionless scheme, with its one-to-one correspondence between source and detection enforced by time-reversal symmetry, could inspire innovative technological developments across various disciplines.

We are grateful to Min Xiao, Fengnian Xia, Qing Gu, Jiazhen Li, Shengwang Du, Yanhua Zhai, and Saeid Vashahri Ghamsari for helpful discussions. This work was partially supported by the NSF ExpandQISE-2329027 and the DoE DE-SC0022069.

* jwen7@binghamton.edu

- [1] T. Young, "I. The Bakerian lecture: Experiments and calculation relative to physical optics," *Philos. Trans. R. Soc.* **94**, 1-16 (1804).
- [2] G. I. Taylor, "Interference fringes with feeble light," *Prof. Cam. Phil. Soc.* **15**, 114-115 (1909).
- [3] W. K. Wothers and W. H. Zurek, "Complementarity in the double-slit experiment: Quantum nonseparability and a quantitative statement of Bohr's principle," *Phys. Rev. D* **19**, 473-484 (1979).
- [4] M. O. Scully, B. G. Englert, and H. Walther, "Quantum optical tests of complementarity," *Nature* **351**, 111-116 (1991).
- [5] P. Storey, S. Tan, M. Collect, and D. Walls, "Path detection and the uncertainty principle," *Nature* **367**, 626-628 (1994).
- [6] B. G. Englert, "Fringe visibility and which-way information: An inequality," *Phys. Rev. Lett.* **77**, 2154-2157 (1996).
- [7] A. Zeilinger, "Experiment and the foundations of quantum physics," *Rev. Mod. Phys.* **71**, S288-S297 (1999).
- [8] Y.-H. Kim, R. Yu, S. P. Kulik, Y.-H. Shih, and M. O. Scully, "A delayed choice quantum eraser," *Phys. Rev. Lett.* **84**, 1-5 (2000).
- [9] R. Mir, J. S. Lundeen, M. W. Mitchell, A. M. Steinberg, J. L. Garretson, and H. M. Wiseman, "A double-slit 'which-way' experiment on the complementarity-uncertainty debate," *New J. Phys.* **9**, 287 (2007).
- [10] S. Kocsis, B. Braverman, S. Ravets, M. J. Stevens, R. P. Mirin, L. K. Shalm, and A. M. Steinberg, "Observing the average trajectories of single photons in a two-slit interferometer," *Science* **332**, 1170-1173 (2011).
- [11] R. Menzel, D. Puhlmann, A. Heuer, and W. P. Schleich, "Wave-particle dualism and complementarity unraveled by a different mode," *Proc. Natl. Acad. Sci. U.S.A.* **109**, 9314-9319 (2012).
- [12] Y. Aharonov, E. Cohen, F. Colombo, T. Landsberger, I. Sabadini, D. C. Struppa, and J. Tollasken, "Finally making sense of the double-slit experiment," *Prof. Natl. Acad. Sci. U.S.A.* **114**, 6480-6485 (2017).
- [13] O. Donati, G. F. Missiroli, and G. Pozzi, "An experiment on electron interference," *Am. J. Phys.* **41**, 639-644 (1973).
- [14] C. Philippidis, C. Dewdney, and B. J. Hiley, "Quantum interference and the quantum potential," *II Nuovo Cimento B* **52**, 15-28 (1979).
- [15] A. Zeilinger, R. Gähler, C. G. Shull, W. Treimer, and W. Mampe, "Single- and double-slit diffraction of neutrons," *Rev. Mod. Phys.* **60**, 1067-1073 (1988).
- [16] A. Tonomura, J. Endo, T. Matsuda, T. Kawasaki, and H. Ezawa, "Demonstration of single electron buildup of an interference pattern," *Am. J. Phys.* **57**, 117-120 (1989).
- [17] O. Carnal and J. Mlynek, "Young's double-slit experiment with atoms: A simple atom interferometer," *Phys. Rev. Lett.* **66**, 2689-2692 (1991).
- [18] M. W. Noel and C. R. Stroud, Jr., "Young's double-slit interferometry with an atom," *Phys. Rev. Lett.* **75**, 1252-1255 (1995).
- [19] M. Arndt, O. Nairz, J. Vos-Andreae, C. Keller, G. van der Zouw, and A. Zeilinger, "Wave-particle duality of C₆₀ molecules," *Nature* **401**, 680-682 (1999).
- [20] H. F. Schouten, N. Kuzmin, G. Dubois, T. D. Visser, G. Gbur, P. F. A. Alkemade, H. Block, G. W. Hooft, D. Lenstra, and E. R. Eliel, "Plasmon-assisted two-slit transmission: Young's experiment revisited," *Phys. Rev. Lett.* **94**, 053901 (2005).
- [21] S. Gerlich, S. Eibenberger, M. Tomandl, S. Nimmrichter, K. Hornberger, P. J. Fagan, J. Tüxen, M. Mayor, and M. Arndt, "Quantum interference of large organic molecules," *Nat. Commun.* **2**, 263 (2011).
- [22] S. Frabboni, A. Gabrielli, G. C. Gazzadi, F. Giorgi, G. Matteucci, G. Pozzi, N. S. Cesari, M. Villa, and A. Zoccoli, "The Young-Feynman two-slits experiment with single electrons: Build-up of the interference pattern and arrival-time distribution using a fast-readout pixel detector," *Ultramicroscopy* **116**, 73-76 (2012).
- [23] J. Pusehouse, A. J. Murray, J. Wätzel, and J. Berakdar, "Dynamic double-slit experiment in a single atom," *Phys. Rev. Lett.* **122**, 053204 (2019).
- [24] Y. Y. Fein, P. Geyer, P. Zwick, F. Kialka, S. Pedalino, M. Mayor, S. Gerlich, and M. Arndt, "Quantum superposition of molecules beyond 25 kDa," *Nat. Phys.* **15**, 1242-1245 (2019).
- [25] W. Lauterborn, T. Kurz, and M. Wiesenfeldt, *Coherent Optics* (Springer Verlag, Germany, 1993).
- [26] L. Zehnder, "Ein neuer interferenzrefraktor," *Zeitschrift für Instrumentekunde* **11**, 275-285 (1891).
- [27] L. Mach, "Ueber einen interferenzrefraktor," *Zeitschrift für Instrumentekunde* **12**, 89-93 (1892).
- [28] P. Grangier, G. Roger, and A. Aspect, "Experimental evidence for photon anticorrelation effects on a beam splitter: A new light on single-photon interferences," *Europhys. Lett.* **1**, 173-179 (1986).
- [29] V. Scarani and A. Surez, "Introducing quantum mechanics: One-particle interferences," *Am. J. Phys.* **66**, 718-721 (1998).
- [30] M. G. A. Paris, "Entanglement and visibility at the output of a Mach-Zehnder interferometer," *Phys. Rev. A* **59**, 1615-1621 (1999).
- [31] D. W. Pohl, W. Denk, and M. Lanz, "Optical stethoscopy: Image recording with resolution $\lambda/20$," *Appl. Phys. Lett.* **44**, 651-653 (1984).
- [32] J. B. Pendry, "Negative refraction makes a perfect lens,"

- Phys. Rev. Lett.* **85**, 3966-3969 (2000).
- [33] M. Minsky, "Memoir on in inventing the confocal scanning microscope," *Scanning* **10**, 128-138 (1988).
- [34] C. Cremer and T. Cremer, "Considerations on a laser-scanning-microscope with high resolution and depth of field," *Microscopica Acta* **81**, 31-44 (1978).
- [35] J. M. Gueera, "Super-resolution through illumination by diffraction-born evanescent waves," *Appl. Phys. Lett.* **66**, 3555-3557 (1995).
- [36] R. Heintzmann, T. M. Jovin, and C. Cremer, "Saturated patterned excitation microscopy a concept for optical resolution improvement," *J. Opt. Soc. Am. A* **19**, 1599-2109 (2002).
- [37] S. W. Hell and J. Wichmann, "Breaking the diffraction resolution limit by stimulated emission: Stimulated-emission-depletion fluorescence microscopy," *Opt. Lett.* **19**, 780-782 (1994).
- [38] M. Hofmann, C. Eggeling, S. Jakobs, and S. W. Hell, "Breaking the diffraction barrier in fluorescence microscopy at low light intensities by using reversibly photo-switchable proteins," *Proc. Natl. Acad. Sci. U.S.A.* **102**, 17565-17569 (2005).
- [39] E. Betzig, G. H. Patterson, R. Sougrat, O. W. Lindwasser, S. Olenych, J. S. Bonifacino, M. W. Davidson, J. Lippincott-Schwartz, and H. F. Hess, "Imaging intracellular fluorescent proteins at nanometer resolution," *Science* **313**, 1642-1645 (2006).
- [40] M. J. Rust, M. Bates, and X. Zhuang, "Sub diffraction-limit imaging by stochastic optical reconstruction microscopy (STORM)," *Nat. Mater.* **3**, 793-796 (2006).
- [41] T. Dertinger, R. Colyer, G. Iyer, S. Weiss, and J. Enderlein, "Fast, background-free, 3D super-resolution optical fluctuation imaging (SOFI)," *Proc. Natl. Acad. Sci. U.S.A.* **106**, 22287-22292 (2009).
- [42] A. N. Boto, P. Kok, D. S. Abrams, S. L. Braunstein, C. P. Williams, and J. P. Dowling "Quantum interferometric optical lithography: Exploiting entanglement to beat the diffraction limit," *Phys. Rev. Lett.* **85**, 2733-2736 (2000).
- [43] Y.-H. Zhai, X.-H. Chen, D. Zhang, and L.-A. Wu, "Two-photon interference with true thermal light," *Phys. Rev. A* **72**, 043805 (2005).
- [44] J. Wen, S. Du, and M. Xiao, "Improving spatial resolution in quantum imaging beyond the Rayleigh diffraction limit using multiphoton W entangled states," *Phys. Lett. A* **374**, 3908-3911 (2010).
- [45] D. V. Strekalov, A. V. Sergienko, D. N. Klyshko, and Y. H. Shih, "Observation of two-photon 'ghost' interference and diffraction," *Phys. Rev. Lett.* **74**, 3600-3603 (1995).
- [46] S. Thanvanthri and M. H. Rubin, "Ghost interference with an optical parametric amplifier," *Phys. Rev. A* **70**, 063811 (2004).
- [47] D. N. Klyshko, "Two-photon light: Influence of filtration and a new possible EPR experiment," *Phys. Lett. A* **128**, 133-137 (1988).
- [48] J. Wen, "Forming positive-negative images using conditional partial measurements from reference arm in ghost imaging," *J. Opt. Soc. Am. A* **29**, 1906-1911 (2012).